Proceedings of Ninth World Conference on Earthquake Engineering
August 2-9, 1988, Tokyo-Kyoto, JAPAN (Vol.IV)

6-6-7

AN EXPERIMENTAL STUDY ON EFFECT OF STRUCTURAL JOINTS ARRANGED IN R/C FRAMES WITH SPANDREL WALLS

Hisahiro HIRAISHI[1], Toshikazu KAWASHIMA[2] and Akiyoshi SATO[3]

[1]Head, Structure Division, Building Research Institute, Ministry of
[2]Construction, Tukuba-shi, Ibaraki, Japan
[2]Research Assistant, Structure Division, Building Research Institute,
[3]MOC, Tukuba-shi, Ibaraki, Japan
[3]Technical Officer of Building Division, Governmental Buildings
Department, MOC, Japan

SUMMARY

The spandrel walls frequently cause brittle failure to the columns. In this paper, seismic tests on beam and column assemblage with spandrel walls were performed in order to investigate the effects of three different types of the week structural joint between the column and spandrel walls. Based on the test results, analytical methods for the strength of such assemblage considering the strength of the structural joints were presented. The paper also proposed the design method to define the dimensions of the structural joints so that the members with spandrel walls might behave in good ductile manner.

INTRODUCTION

Spandrel walls are usually used in buildings such as a school and a hospital. They stiffen the structures. However, severe shear failure of columns have occurred during earthquakes due to the existence of the spandrel walls, which frequently have caused brittle failure of whole structure. Recently, the structural design method arranging the week structural joint (hereafter refferred to as the "slit") between a column and spandrel walls has been adopted to prevent such brittle failure of columns with spandrel walls and to improve the ductility of the structure against earthquakes. "Structural Design Guide and Commentary,"[1] published by Japan Building Center describes that the spandrel walls need not be taken into consideration in the structural design if the thickness of the spandrel wall is less than 10cm, and the ratio of its thickness to the column width is less than 1/6. However, some researches have pointed based on the experimental results that such description is not reasonable.[2] This paper proposes the analytical method to estimate the strength of the slit and the design method of the slit, based on the experimental results of beam-column and spandrel wall assemblage with the slits.

OUTLINE OF EXPERIMENTS

The specimens were half-scale models representing a second floor beam-column and spandrel wall assemblage of a four-story school building. The variable is the detail of the slit between the column and the spandrel walls. The details of reinforcement are shown in Fig. 1. The dimensions of the slit of each specimen are listed in Table 1 and the details of the slits (Type I, II and III) are shown in Fig. 2. The material properties of reinforcing bars and concrete are listed in Table 2, and the stress versus strain curves of concrete obtained by the

compressive cylinder tests are shown in Fig. 3 by the dotted lines together with the two analytical relations shown by the solid lines used later.

The test set-up is illustrated in Fig. 4. The top and bottom ends of the column were supported by the pin-roller, respectively. The constant axial load (average axial stress of 20 kg/cm^2) was applied to the top of the column. Both ends of beams were deformed in the opposite direction each other with the same vertical displacement amplitude by the hydraulic jacks.

TEST RESULTS

The relationship between the story shear and the story displacement of the test results, and the specimens after test are shown in Figs. 5 and 6 as to Specimens SW-B, SW-D, and SW-E.

The similar sequence of cracking, crushing and yielding was observed for Specimens SW-A, SW-B, SW-C and SW-D. When the story drift angle (the story displacement divided by the column height) reached about 1/300rad., the concrete of the slit crushed and the story shear decreased. After that, the beam yielded, then the specimens showed the stable spindle-type hysteresis loop without any deterioration in strength even in large deformation range. The remarkable cracks concentrated only in the beams. The spandrel walls themselves was not damaged severely. The slit of Type II failed in shear due to the compression stress by flexure of the beam at the extremely small story drift angle.

As for Specimen SW-E, the slit also crushed before the beam formed hinge. After the longitudinal steel bars of the beams yielded, pinching of the loops was observed due to the bond slippage between the logitudinal steel bars arranged in the beams and concrete in the joint, and the damage on the joint was severer, because the column width of Specimen SW-E was smaller than those of the other specimens.

The story drift angle at the failure of the slit of Types II and III was much larger than that at the failure of the slit of Type-II in Specimen SW-D.

ANALYSIS OF STRENGTH OF SLITS

Slit of Type I The seaquence of cracking and crushing and the final appearance of concrete of the slits of Type I suggested that the slits failed in compression due to flexure in beam (see Fig. 7). Figure 8 shows the average strains at several different heights of the slit normalized by the average strain at the top of the slit together with three parabolic lines. These strains are based on the measured lateral displacements between both faces of the column and the spandrel wall around the maximum bending strength of the beam. The relations given by Eq. (1) gives the good corelation with the test results of the strain distributions along the height of the slit. The idealized deflection profile of the specimens and the idealized distribution of compressive stress of the slit are illustrated in Fig. 7. The working resultant force in the slit is given by Eq. (2). The bending moment at the critical section of the beam is given by Eq. (3) assuming that any axial compression stress does not occur in the beam and tensile stress occurs only in the bottom longitudinal steel bars.

$$\varepsilon_\eta = \varepsilon_c \cdot \eta^{3/2} \tag{1}$$

$$C = t \cdot h_s \cdot \int_0^1 \sigma_\eta \, d\eta = \alpha \cdot t \cdot h_s \cdot {}_c\sigma_B \tag{2}$$

$$M = C\,(j_C + j_T) = \alpha_M \cdot t \cdot h_s \cdot j_T \cdot {}_c\sigma_B \tag{3}$$

$$\alpha_M = \alpha\,(j_C / j_T + 1) \tag{4}$$

where :

ε_η, ε_c, η, σ_η = notation shown in Fig. 7,

α = coefficient of strength of slit,
t = thickness of slit,
h_s = height of spandrel wall,
$_c\sigma_B$ = compressive strength of concrete,
j_c = distance from the upper surface of the beam to the location of the working resultant force, and
j_T = distance from the upper surface of the beam to the bottom longitudinal bars in the beam.

As a result, the bending moment is given as the function of ε_c. Table 3 lists the analytical and test results of the maximum bending moment in the critical section of the beam. The analytical results expressed by Cal. 1 are calculated by the fiber model method assuming that the plain section at the critical section remains plain after bending. The analytical results expressed by Cal. 2 are the maxima of the bending moment M_{max} given by Eq. (3), and those expressed by Cal. 3 are calculated by the approximate equation given by Eq. (5). The stress versus strain relation of Case 2 shown in Fig. 3 is used in Cal. 1 and Cal. 2. Cal. 2 and Cal. 3 show the excellent agreement with the test results, while Cal. 1 using the hyposthesis of a plain section remaining plain overestimates the test results. The approximate equation for Eq. (3) at the maximum of the bending moment is given by Eq. (5). Here, the compressive strength of concrete is limited from 120 kg/cm^2 to 270 kg/cm^2, the relation of Case 2 in Fig. 3 is used as the stress versus strain relation of concrete, and j_T is assumed to 0.9d (d: effective depth of the beam).

$$M_{max} = 0.9\ \alpha_{Mmax} \cdot t \cdot h_s \cdot d \cdot j_T \cdot {}_c\sigma_B \tag{5}$$

$$\alpha_{Mmax} = 0.80 + 0.44\ h_s / d - 0.0007\ {}_c\sigma_B \tag{6}$$

Slit of Type III The maximum moment at the critical section of the beam is expressed by Eq. (7) where it is assumed that only the slit of Type III trnsfers compression force and only the bottom longitudinal steel bars does tension force.

$$M_{max} = C_3 \cdot j_3 \tag{7}$$

where : C_3 = lateral compressive strength of slit of Type III ($=A_e \cdot {}_c\sigma_B$),
A_e = vertical sectional area of slit of Type III, and
j_3 = distance from the bottom longitudinal steel bars of beam to the center of slit of Type III

Table 4 listed the analytical and test results of the maximum bending moments at the critical section of the beam. The analytical results expressed by Cal. 1 are calculated by fiber model method where 1/6 of the effective cross sectional area on shear of the slit of Type II is considered as the equivalent cross sectional area to that of the slit of Type I. The analytical results expressed by Cal. 2 are calculated by Eq. (7) where the compressive strength of concrete of 1.2 times the strength of the cylinder test is used as that of the slit of Type II by considering the increase in strength due to its aspect ratios of the shape of the slit of Type III. In these calculations, the reinforcing steel bars crossing the slits are considered while those in the slit of Type II are not. Both analytical results show good agreement with the test results.

PROPOSAL FOR DESIGN OF SLITS

Generally speaking, slits fail in compression due to the bending moment at the critical section of beams. Therefore, the following design procedure is recommended in order that the failure of the slits occur prior to yielding of the beams and columns without any increase in the maximum strengths of the beams and columns themselves due to spandrel walls :

(a) calculation of the bending moment (M_m) at the critical section of the beam at hinge mechanism of the structure by ignoring spandrel walls, and

(b) define the dimensions of the slits by Eq. (8).

$$M_m > M_{max} \tag{8}$$

where M_{max} is the maximum bending moment of the beam with the spandrel wall given by Eqs. (5) and (7), for the slits of Types I and III, respectively. Equation (5) is rewritten as the simple approximate equation given by Eq. (9).

$$M_{max} = C_1 \cdot j_1 \tag{9}$$

where :

$$C_1 = \alpha \cdot t \cdot h_s \cdot {}_c\sigma_B \tag{10}$$

$$j_1 = 0.65 h_s + d \tag{11}$$

$$\alpha = 0.65 \text{ (when only column forms hinge)} \tag{12}$$
$$0.70 \text{ (when beam forms hinge)}$$

If the beam is sufficiently stiff and strong as foundation beams, the failure of the slit is caused by shear produced in the column. In this case, the dimensions of the slit should be defined as follows :

(a) calculate the shear (Q_c) of the column at hinge mechanism of the structure by ignoring spandrel walls, and

(b) define the dimensions of the slit by Eq. (13).

$$Q_c > C_{max} \tag{13}$$

where : C_{max} = strength of slit given by substituting Eq. (12) into Eq. (10)

If the following Equation (14) is satisfied the bending moment after yielding of bottom longitudinal steel bars of the beam with spandrel wall is the same as the maximum bending moment (M_y) of the beam itself although strength of the beam with the spandrel wall temporarily exceed before the concrete of the slits completely crushs.

$$T_b > C_{max} \tag{14}$$

where T_b is the yield strength of the bottom longitudinal steel bars in the beam.

CONCLUSIONS

The following findings were drawn from this study.

(1) The slits of Types I and III generally fails in compression due to bending moment at the critical section of the beam.

(2) The influence of spandrel walls having the slit of Type II on the seismic behavior is negligible.

(3) The analytical strengths considering the strength of the slits agreeds well with the test results.

(4) The dimension of the slit is defined by the proposed simple equations so that the members with spandrel walls might behave in good ductile manner.

ACKNOWLEDGMENT

The authors would like to express their sincere thanks to Miss N. Ishikawa for her editing the manuscript.

REFERENCES

1. Japan Building Center, "Structural Design Guide and Commentary," (1986), (in Japanese).
2. Kano, Y., et al., "Study on Effect of Reinforced Concrete Column Confined by Spandrel Wall," Summaries of Technical Papers of Annual Meeting of AIJ, Aug., (1986), (in Japanese).
3. Kent, D.C., Park, R.,"Flexural Members with Confined Concrete," Proc. of ASCE, Vol. 97, St 7, July., (1971).
4. Hiraishi, H., Sato, A., et al., "Study on Effect of Slit on Reinforced Concrete Column-Spandrel Wall Assemblage," Trans. of AIJ, No. 362, Apr., (1986), (in Japanese).

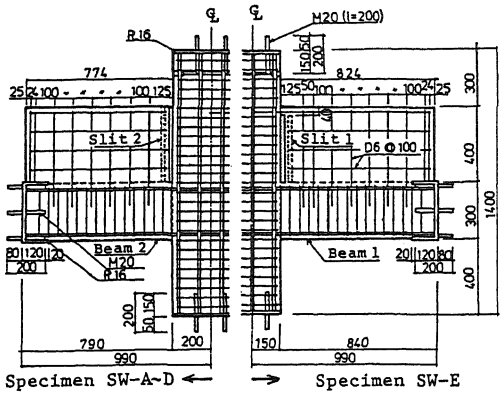

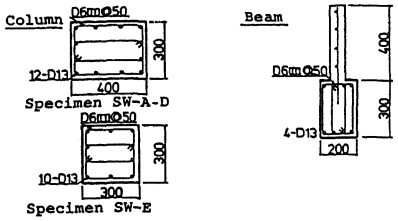

Fig. 1 Details of Reinforcement

Table 1 Dimensions of Slits

Specimen		Slit Type	Dimension (mm) t	Δ	d_s*1
SW-A	Slit 1	Type I	25(27)	50	—
	Slit 2	Type I	20(19)	40	—
SW-B	Slit 1	Type I	35(36)	70	—
	Slit 2	Type I	30(32)	60	—
SW-C	Slit 1	Type III	80	60	40
	Slit 2	Type II + III	80*2	60*2	40*2
SW-D	Slit 1	Type III	60	60	60
	Slit 2	Type II	—	—	—
SW-E	Slit 1	Type II + III	80*2	60*2	40*2
	Slit 2	Type I	25	50	—

( ): measured size *1: depth of slit of Type III
*2: dimension with respect to Type III

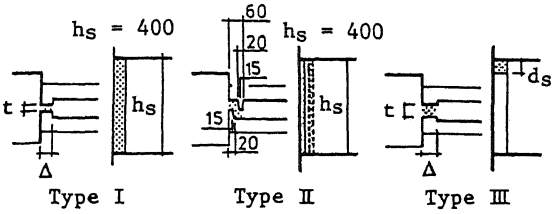

Fig. 2 Types of Slit

Table 2 Material Properties

(a) reinforcing bars

Specimen	Bar	$_s\sigma_y$ (kg/cm2)	$_s\sigma_{max}$ (kg/cm2)	E_s (kg/cm2)
SW-A,B	D13	3,850	5,530	1.76×10^6
	D6	3,860	5,520	1.86×10^6
SW-C-E	D13	3,740	5,400	1.81×10^6
	D6	3,920	5,650	2.04×10^6

$_s\sigma_y$: Yeild Strength
$_s\sigma_{max}$: Tensile Strength
E_s : Elastic Modulus

(b) concrete

Specimen	$_c\sigma_B$ (kg/cm2)	E_c (kg/cm2)	$_c\sigma_T$ (kg/cm2)
SW-A,B	212	1.92×10^5	21.2
SW-C-E	234	2.52×10^5	21.1

$_c\sigma_B$: Compressive Strength
E_c : Elastic Modulus
$_c\sigma_T$: Tensile Strength

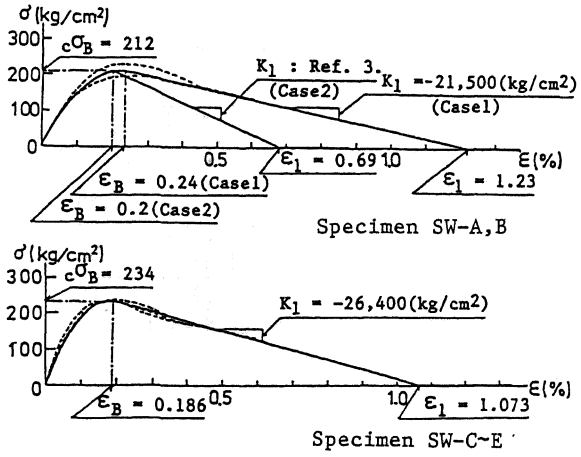

Fig. 3 Stress-Strain Relations of concrete

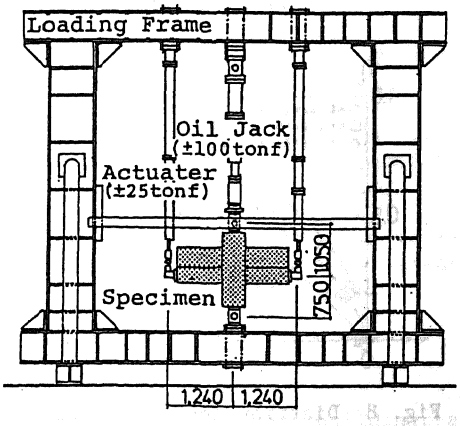

Fig. 4 Test Set-up

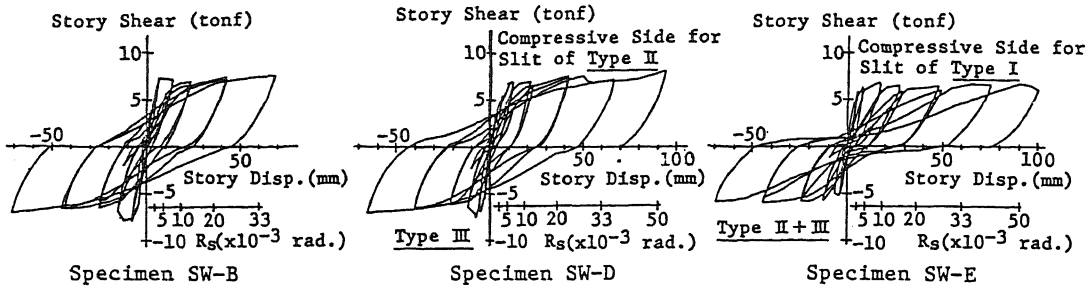

Fig. 5 Relation between Story Shear and Story Displacement

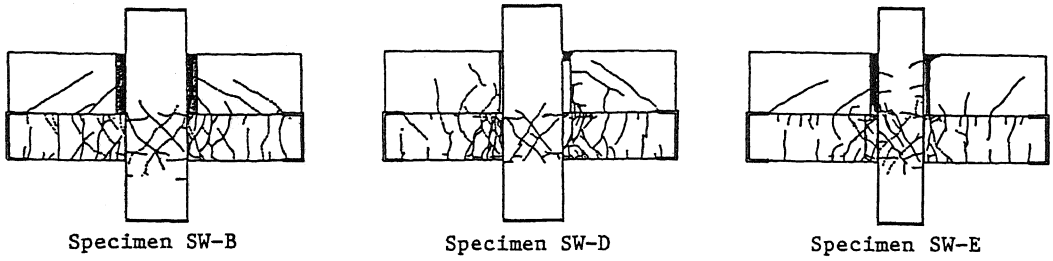

Fig. 6 Specimen after Test

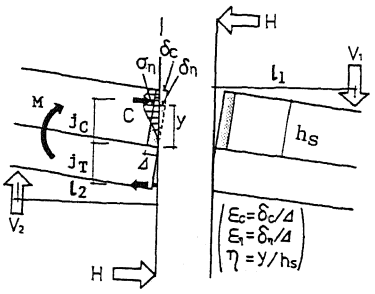

Fig. 7 Deflection and Stress of Slit

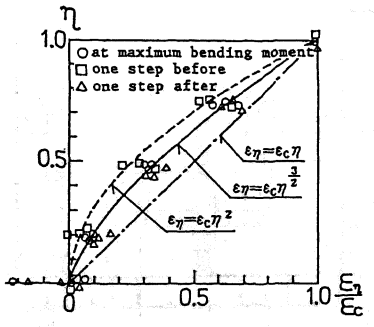

Fig. 8 Distribution of lateral Compressive Strain along Height of Slit

Table 3 Maximum Bending Moment at Column Face (Slit of Type I)

Specimen		Cal.1 *1 M(ton m)	Cal.2 *2 M(ton m)	Cal.3 *3 M(ton m)	Ex. M(ton m)
SW-A	Slit 1	9.28(0.82)	7.56(1.01)	7.33(1.04)	7.63
	Slit 2	———	5.31	5.16	———
SW-B	Slit 1	10.8(0.90)	10.1(0.97)	9.78(1.00)	9.76
	Slit 2	10.2(0.81)	8.95(0.93)	8.69(0.96)	8.33
SW-E	Slit 2	9.33(0.69)	7.83(0.83)	7.34(0.88)	6.46

*1 : calculated by Fiber Model Method
*2 : calculated by Eq.(3) *3 : calculated by Eq.(5)
( ): Ex./Cal.

Table 4 Maximum Bending Moment at Column Face (Slit of Type III)

Specimen		Cal.1 *1 M(ton m)	Cal.2 *2 M(ton m)	Ex. M(ton m)
SW-C	Slit 1	7.43(0.87)	6.43(1.00)	6.45
	Slit 2	8.11(0.94)	6.43(1.18)	7.59
SW-D	Slit 1	7.74(0.97)	7.05(1.06)	7.49
SW-E	Slit 1	8.61(0.82)	6.43(1.10)	7.09

*1 : calculated by Fiber Model Method
*2 : calculated by Eq.(7)
( ): Ex./Cal.